

ETV4 Mutation in a Patient with Congenital Anomalies of the Kidney and Urinary Tract

Jing Chen^{1, 2, #}, Amelie T. van der Ven^{1, #}, Joseph A. Newman³, Asaf Vivante^{1, 4}, Nina Mann¹, Hazel Aitkenhead³, Shirlee Shril¹, Hadas Ityel¹, Julian Schulz¹, Johanna Magdalena Schmidt¹, Eugen Widmeier^{1, 5}, Opher Gileadi³, Frank Costantini⁶, Shifaaan Thowfeequ⁶, Roland H. Wenger⁷, Stuart B. Bauer⁸, Richard S. Lee⁸, Weining Lu⁹, Maike Getwan⁵, Michael M. Kaminski⁵, Soeren S. Lienkamp^{5, 10}, Richard P. Lifton^{11, 12}, Velibor Tasic¹³, Elijah O. Kehinde¹⁴ and Friedhelm Hildebrandt^{1, *}

¹Department of Medicine, Boston Children's Hospital, Harvard Medical School, Boston, Massachusetts, USA

²Department of Nephrology, Children's Hospital of Fudan University, Shanghai, China

³The Structural Genomics Consortium, University of Oxford, Old Road Campus Research Building, Oxford, United Kingdom

⁴Talpiot Medical Leadership Program, Sheba Medical Center, Tel-Hashomer, Israel

⁵Department of Medicine, Renal Division, Medical Center – University of Freiburg, Faculty of Medicine, University of Freiburg, Freiburg, Germany

⁶Department of Genetics and Development, Columbia University Medical Center, New York, New York, USA

⁷Institute of Physiology and Zürich Center for Integrative Human Physiology (ZIHP), University of Zürich, Zürich, Switzerland

⁸Department of Urology, Boston Children's Hospital, Harvard Medical School, Massachusetts, USA

⁹Renal Section, Department of Medicine, Boston University Medical Center, Boston, MA, USA

¹⁰Center for Biological Signaling Studies (BIOSS), Freiburg, Germany

¹¹Department of Human Genetics, Yale University School of Medicine, New Haven, CT, USA

¹²Howard Hughes Medical Institute, Chevy Chase, Maryland, USA

¹³Medical Faculty Skopje, University Children's Hospital, Skopje, Macedonia

¹⁴Division of Urology, Department of Surgery, Nazarbayev University, Astana, Kazakhstan

Abstract: Congenital anomalies of the kidney and urinary tract (CAKUT) are the most common reason for chronic kidney disease in children. Although more than 30 monogenic causes have been implicated in isolated forms of human CAKUT so far, the vast majority remains elusive. To identify novel monogenic causes of CAKUT we applied homozygosity mapping, together with whole exome sequencing, in a patient from consanguineous descent with isolated CAKUT. We identified a homozygous missense mutation (p.Arg415His) of the *Ets Translocation Variant Gene 4 (ETV4)*. The transcription factor *ETV4* is a downstream target of the GDNF/RET signaling pathway that plays a crucial role in kidney development. We show by means of electrophoretic mobility shift assay that the Arg415His mutant causes loss of the DNA binding affinity of *ETV4* and fails to activate transcription in a cell-based luciferase reporter assay. We furthermore investigated the impact of the mutant protein on cell migration rate. Unlike wildtype *ETV4*, the Arg415His mutant failed to rescue cell migration defects observed in two *ETV4* knock-down cell-lines. We therefore identified and functionally characterized a recessive mutation in *ETV4* in a human patient with CAKUT. We hypothesize that the pathomechanism of this mutation could be *via* loss of the transcriptional function of *ETV4*, and a resulting abrogation of GDNF/RET/*ETV4* signaling pathway.

Keywords: CAKUT, cell migration, DNA binding, ETS domain.

1. INTRODUCTION

Congenital anomalies of the kidney and urinary tract (CAKUT) encompass a wide spectrum of urinary tract

malformations involving the kidney (e.g. renal agenesis, hypodysplasia) and the urinary tract (e.g. vesicoureteral reflux (VUR), ureteropelvic junction obstruction (UPJO)) [1]. These disorders belong to the most common birth defects and constitute the main cause of chronic kidney disease in children (~50%) [2-4].

*Address correspondence to this author at the Boston Children's Hospital, Division of Nephrology, 300 Longwood Avenue, EN561, Boston, MA 02115, USA; Tel: +1 617-355-6129; Fax: +1 617-730-0569; E-mail: Friedhelm.Hildebrandt@childrens.harvard.edu

It has been hypothesized that single-gene mutations may cause CAKUT in humans [5]. To date, over 30 monogenic causes have been described to lead to CAKUT [6]. Many of these genes show a dominant mode of inheritance [6], yet a significant proportion of recessive genes has been previously implied to cause CAKUT as well (e.g., *ITGA8* and *FGF20*) [7, 8]. In >80% of cases, the causative gene remains to be elucidated [6, 9-12]. Genetic research in CAKUT is complicated by a distinct heterogeneity (>30 genes explain less than 20% of cases), incomplete penetrance and variable expressivity of the phenotype. Mouse models have been helpful in the past for improving the knowledge about the pathogenesis and genetics underlying CAKUT. Screenings for mutations in mouse CAKUT genes have revealed that a significant proportion can be identified in human CAKUT patients [7, 11].

Here, we identify by whole-exome sequencing (WES) a recessive missense mutation in the *ETS translocation variant 4 (ETV4)*; also known as PEA3 or E1AF) in a consanguineous patient with CAKUT. *ETV4* belongs to the E26 transformation-specific (ETS) transcription factor family [13]. *ETV4* has been identified to act downstream of the GDNF/RET signaling pathway, which plays essential roles in kidney development [14]. *ETV4* has previously been shown to be important for migration of progenitor cells during renal branching morphogenesis [15] and is a known cause of CAKUT in mice and zebrafish [14, 16].

2. MATERIALS AND METHODS

2.1. Human Subjects

We obtained blood samples, pedigree, and clinical information after receiving informed consent (<http://renalgenes.org>) from the respective proband with CAKUT. The diagnosis of CAKUT was made by (pediatric) nephrologists and / or urologists based on published clinical criteria. Approval for experiments on humans was obtained from the Institutional Review Boards of Boston Children's Hospital, and local IRBs according to the Declaration of Helsinki.

2.2. Whole-Exome Sequencing, Homozygosity Mapping and Mutation Calling

Whole-exome sequencing (WES) and a variant burden analysis were performed as described previously [17]. Briefly, genomic DNA was isolated from blood lymphocytes and subjected to exome capture using Agilent Sure Select™ human exome capture

arrays (Life Technologies) followed by next generation sequencing on the HiSeq Illumina sequencing platform. Homozygosity mapping was generated from VCF files using Homozygosity Mapper [18]. Sequence reads were mapped against the human reference genome (NCBI build 37/hg19) using CLC Genomics Workbench (version 6.5.1) software (CLC bio). Variants with minor allele frequencies <1% in the dbSNP (Version 142) database were selected and annotated for impact on the encoded protein and for conservation of the reference base and amino acid among orthologs across phylogeny. Variants were filtered on the basis of an autosomal recessive mode of inheritance. Identified mutations were confirmed by Sanger sequencing of genomic DNA.

2.3. High-Throughput *ETV4* Mutation Analysis

Target sequencing of all coding exons and adjacent splice sites of *ETV4*, as well as its 2 interaction partners (*STK11* and *SMAD2*) [19, 20], was performed in 864 individuals from 589 different families with CAKUT from different pediatric nephrology centers worldwide using microfluidic technology (Fluidigm) with subsequent next-generation sequencing as described previously [21]. PCR primer sequences are available upon request. Variants were confirmed by Sanger sequencing, and tested for segregation with the CAKUT phenotype.

2.4. cDNA Cloning

Human full-length *ETV4* cDNA was subcloned from human full-length cDNA clone (NM_001986.2, clone ID: HsCD00326736) (DF/HCC DNA Resource Core, Boston, MA) and the resultant plasmid was used for the generation of the *ETV4* mutant (p.Arg415His) by Quick change II XL site-directed mutagenesis kit (Agilent Technologies, Santa Clara, CA). The sequence was verified *via* Sanger sequencing. The cDNAs for human wild-type and mutant *ETV4* were cloned into pRK5-N-Myc expression vector using LR clonase (Invitrogen, Carlsbad, CA) following the manufacturer's instruction.

2.5. Cell Culture

All cells used in this study were purchased from the ATCC biological resource center. HEK293T cells and U-2 OS cells were cultured in Dulbecco's modified Eagle's medium (DMEM). PC3 cells were grown in Roswell Park Memorial Institute medium (RPMI-1640). Media were supplemented with 10% fetal bovine serum (FBS) and antibiotics (penicillin 100 U/ml and streptomycin 100µg/ml). PC3 and U-2 OS cell lines

with shRNA-mediated stable *ETV4* knock-down were selected and maintained with 4µg/ml puromycin (Life Technologies, Grand Island, NY).

2.6. Electrophoretic Mobility Shift Assay

The dsDNA probe contained the single consensus Ets-binding site (underlined), with oligonucleotides forward (5'- ATCTCACCGGAAGTGTAGCA -3') and reverse (5'- TGCTACACTTCCGGTGAGAT -3'). Substrates were prepared by ³²P-5'-end-labeling one oligonucleotide, annealing to the complementary strand in 10mM Tris-HCl, pH 7.5, 50mM NaCl, prior to purification with Micro Bio-Spin® P-6 columns. Proteins were incubated 30min at room temperature in 50mM Tris-HCl, pH 7.5, 50mM arginine-HCl, pH 7.5, 25mM NaCl, 5% glycerol, 0.01% tween-20 with 0.02nM final ³²P-labeled probe and protein concentrations ranging from 0.025 to 12nM. DNA-protein complexes were separated on 12% polyacrylamide gel with 0.5xTBE. Images were obtained and quantitated using the BioRad Personal Molecular Imaging system (Bio-Rad Laboratories, Hercules, CA) and the binding isotherm was calculated using Graph Pad Prism.

2.7. Luciferase Reporter Assays

The pGL3-5x*ETV4*-Luc reporter plasmid (kindly provided by Andrew Sharrocks [22]), contains 5 copies of *ETV4*/ETS binding sites and AdML promoter, and has been described previously [23]. HEK293T cells were seeded into 24-well plates with density of 50,000 cells per well. 24h after plating, at about 75% confluence the cell were co-transfected with 300ng wild-type or mutant pRK5-N-Myc-*ETV4*, 200ng pGL3-5x*ETV4*-Luc, and 40ng pCS2 Renilla luciferase (Promega, Madison, WI). Plasmid transfections for HEK293 cells were performed with Lipofectamine 2000 transfection reagent (Invitrogen, Carlsbad, CA) according to the manufacturer's instructions. Cells were harvested 48h after transfection. Firefly and renilla luciferase levels were assayed with the dual-luciferase reporter assay system (Promega, Madison, WI) using a GloMax microplate luminometer with dual injectors (Promega, Madison, WI). The activity of firefly luciferase was normalized to that of renilla luciferase. After normalization, the mean luciferase activities and standard deviations were plotted as "fold activation" when compared with the empty expression plasmid. All transfections were performed in triplicate, and individual experiments were repeated in duplicate. Statistical analysis was performed with a two-tailed Student t-test using GraphPad Prism®. $P < 0.05$ was considered statistically significant.

2.8. Retroviral Infections and Stable Selection

ShRNA against human *ETV4* was subcloned into pSIREN-RetroQ for retroviral transduction using HEK293T cells. 48 hours after transduction puromycin at a final concentration of 4µg/ml was added to the medium for selection of transduced PC3 or U-2 OS cells. Target sequence of *ETV4* shRNA is GCTGCCCTGTGTACATATAAA (Region: 3'UTR). See Figure 3a-d for knockdown efficiency.

2.9. Western Blot Analysis

For the Western blot assay, whole cell protein was extracted from PC3 cells with RIPA buffer supplemented with protease inhibitors and phosphatase inhibitor cocktail (Thermo Scientific, Rockford, IL); nuclear protein was isolated extracted from U-2 OS cells using NE-PER® Nuclear and Cytoplasmic Extraction Reagents (Thermo Scientific, Rockford, IL). Protein concentration was determined by the DC protein assay (Bio-Rad Laboratories, Hercules, CA) and equivalent amounts of protein were electrophoresed on NuPAGETM NovexTM 4-12% Bis-Tris gels (Invitrogen, Carlsbad, CA). Prestained Protein Ladder was used to determine relative molecular weights. The gels were electro blotted onto PVDF membranes using iBlot® Dry Blotting System (Invitrogen, Carlsbad, CA). After blocking with 5% defatted milk powder, membranes were incubated with the following anti-human antibodies: mouse monoclonal antibody (mAb) anti-*ETV4* (clone 3G9-1B9, Abnova, Taipei, Taiwan), mAb anti-beta-actin (ab20272, Abcam, Cambridge, MA), mAb anti-PCNA (ab18390, Abcam, Cambridge, MA). Except for mAb anti-beta-actin, primary antibodies were detected with donkey anti-mouse sera conjugated to horseradish peroxidase (sc-2314, Santa Cruz Biotechnology, Dallas, TX). Chemiluminescent signals were developed using Super Signal West Pico substrate or SuperSignal West Dura substrate (Thermo Scientific, Rockford, IL). The images were acquired with ChemiDocTM MP Imaging System (Bio-Rad Laboratories, Hercules, CA).

2.10. Quantitative Polymerase-Chain Reaction

RNAs of U-2 OS and PC3 cells were isolated using the RNeasy Plus Mini Kit (Qiagen, Valencia, CA) following the manufacturer's instructions. RNA was subsequently converted into cDNA using the iScript cDNA synthesis kit (Bio-Rad Laboratories, Hercules, CA).

Quantitative real time PCR was performed using TaqMan® reagents (Applied Biosystem, Foster City,

CA) following the manufacturer's instructions. Expression values of human *ETV4* were normalized against expression levels of human *GAPDH*. Results are plotted as relative mRNA levels. Error bars indicate the standard deviation of the mean. Each experiment was performed in triplicate.

2.11. Migration Assay

Real-time migration assays were performed using the Incucyte System (Essen Instruments, Ann Arbor, MI). Immortalized human osteosarcoma (U-2 OS) and prostate cancer (PC3) cells with shRNA-mediated knockdown of *ETV4* were transfected with MOCK-Myc, N-myc *ETV4*-WT or N-myc *ETV4*-Arg415His. Mirus IT-LT (Mirus Bio LLC, Madison, WI) (U-2 OS) and Lipofectamine 2000 (PC3) were used as transfection reagents following the manufacturer's instructions. 48 hours after the transfection, 30,000 cells (U-2 OS) / 35,000 cells (PC3) were seeded onto a 96-well Image Lock Plate. After 6-12 hours, 100% confluent cells were wounded using a semi-manual wound-maker tool. Cells were subsequently cultured in cell-specific media supplemented with 15% FBS. Cells with non-target control shRNA (unspecific knock-down) served as control. Serum-free media was added to a subset of wells with non-target control shRNA as negative control.

Images and measurements of the created wounds were taken every hour for up to 20 hours applying around-the-clock kinetic imaging. Changes in wound confluence were calculated using the Incucyte System (Essen Instruments). Results are plotted as wound width (%) over time (h). Each condition was performed in triplicate, experiments were repeated two times independently. Changes in wound width are presented as means with \pm SD.

3. RESULTS

3.1. Identification of the Arg415His *ETV4* Mutation in a CAKUT Patient

To identify additional CAKUT-causing genes, we performed WES in an individual of Kuwaiti ancestry with isolated CAKUT (Figure 1a and 1d). Homozygosity mapping revealed 173 Mb of total homozygosity indicating a close relationship of both parents, potentially to the degree of first cousins. Given the parent's consanguinity as well as the unaffected status in regards to CAKUT, we hypothesized a recessive mode of inheritance. Among the homozygous missense variants identified (filtering strategy outlined

in methods section and Table 1), five were successfully confirmed by Sanger sequencing of the patient's DNA and were shown to be heterozygous in the maternal DNA. *ETV4* was subsequently prioritized due to its known involvement in the development of the kidney and urinary tract and corresponding animal models with CAKUT [14, 15, 24].

The index patient had right-sided grade II vesicoureteral reflux (VUR) (Figure 1b) for which she required a subureteral injection of Teflon at the age of 5 years. This treatment resulted in a complete resolution of VUR as shown by a subsequent voiding cystourethrogram (Figure 1c). In the patient, we detected a homozygous missense mutation in position chr17: 41606098; c.1244G>A in exon 13 of the *ETV4* gene (NM_001079675.2). This homozygous missense mutation (rs373515634) results in the amino-acid change p. Arg415His. The healthy mother was heterozygous for the p. Arg415His mutation confirming her carrier status (Figure 1e).

Arginine 415 is an *ETV4* encoded residue that is well conserved across species including *C. elegans* and of all *H. sapiens* ETS paralogous proteins (Figure 1f and 1g) which is also reflected by conservation scores of 1.00 and 6.42 in phastCons and phyloP, respectively. The *ETV4* mutation was predicted to be 'disease causing' by the Mutation Taster software, 'deleterious' in SIFT (see URLs) and to date has never been reported homozygously in the healthy population (in regards to CAKUT) in the Exome Variant Server, the 1 000 Genomes Project and the Exome Aggregation Consortium (see URLs).

The patient's DNA was additionally screened for mutations in 36 established CAKUT causing genes including *RET*, *PAX2*, *HNF1 β* , *EYA1*, *SIX1*, and copy number variations in *HNF1 β* without results [6].

We performed targeted sequencing of all exons of *ETV4* and its 2 interaction partners (*STK11* and *SMAD2*) in a worldwide cohort of 864 individuals from 589 different families with CAKUT, but were not able to detect any additional CAKUT families with mutations in either of these 3 genes [19, 20].

3.2. The Arg415His *ETV4* Mutant Abrogates DNA Binding Affinity of *ETV4*

ETV4 encodes the ETS family transcription factor Ets variant 4. It belongs to the ETS gene family, a large group of transcription factors involved in diverse aspects of embryonic development. The *ETV4* protein

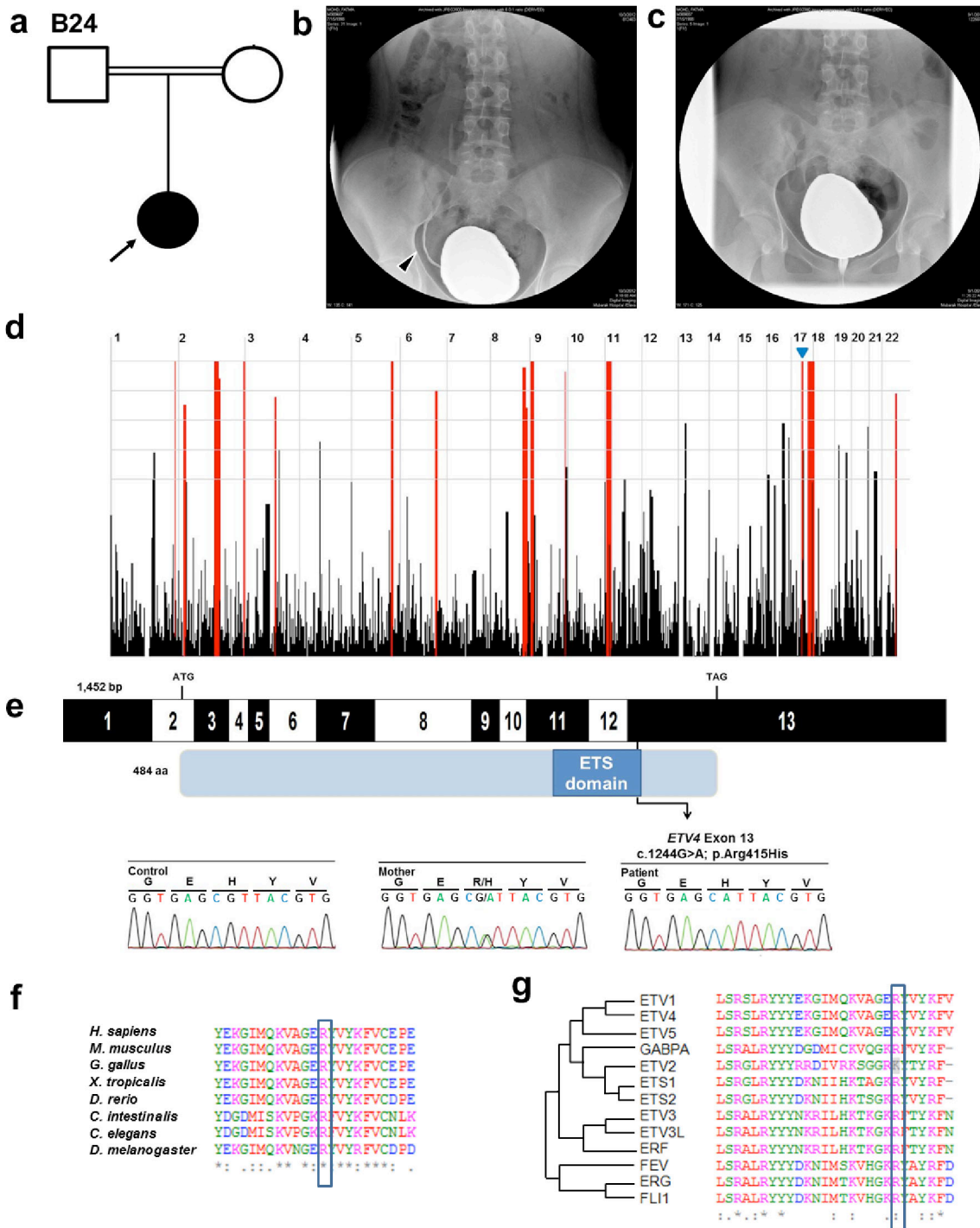


Figure 1: Identification of a recessive mutation in *ETV4* in family B24 with CAKUT. **(a)** Pedigree of index family B24. Squares represent males, circles females, black symbol indicates the affected patient and white symbols the unaffected parents. Double horizontal lines denote consanguineous marriage. The black arrow points to the proband B24-21. **(b)** Voiding cystourethrography of patient B24-21 with reported right grade II vesicoureteral reflux (VUR). The image shows reflux into the ureter (white arrowhead). Images demonstrating a reflux into the kidney could not be obtained. **(c)** Follow-up voiding cystourethrography shows complete resolution after subureteral transurethral injection (STING). **(d)** Homozygosity mapping identifies recessive candidate loci (red peaks) in family B24 with CAKUT, and whole-exome sequencing identifies a homozygous mutation in *ETV4* (positioned at blue arrowhead). **(e)** The exon (black and white) and protein domain (blue) structures of human *ETV4* cDNA. Positions of start codon (ATG) and of stop codon (TAG) are indicated. The arrow indicates the position of *ETV4* mutation in relation to exons and protein domain. Chromatograms obtained by direct sequencing of PCR products reveal a homozygous substitution of A for G in exon 13 of the *ETV4* gene in the patient, and heterozygous mutation in the patient's mother. **(f)** Amino acid sequence conservation among species of p.Arg415His that was altered in *ETV4* of patient B24-21 with CAKUT. The arginine residue in this position is well conserved throughout evolution. **(g)** Amino acid residue Arg415 is highly conserved in 11 of all 12 different human *ETV4* paralogs. In *ETV2* it is replaced by another positively charged residue, K.

Table 1: Filtering Process for Variants from hg19 Reference Sequence Following WES in Individual from Consanguineous Descent and Isolated CAKUT

Family	B24
Affected Individual Sent for WES	B24-21
Consanguinity	Yes
^a # of homozygosity peaks	37
Cumulative Homozygosity by descent [Mb]	173
^b Hypothesis from mapping: homozygous (H), heterozygous (h)	H
Total sequence reads (Mill.)	75
Matched Reads	73
total # of variants detected	404,794
Reject common dbSNP142, MAF >1%	86,042
Keep VF>55% AND Cov >=2	46,639
Non-synonymous and Splice	1262
Located in hom peaks	83
(Located within splice site)	8
(Deletion/Insertion)	4
(Stop gained/stop lost)	0
(Missenses)	71
Surviving variants after inspection	8
Sanger confirmation/Segregation	5
Causative gene	ETV4
Mutation effect on gene product	R415H (H)

^aSee Figure 1.

^bEvaluation for homozygous variants was done in regions of homozygosity by descent.

WES: Whole exome sequencing; CAKUT: Congenital anomalies of the kidney and urinary tract; SNP: Single nucleotide polymorphism; MAF: Minor allele frequency.

contains an evolutionarily conserved ETS DNA-binding domain shared by all ETS family proteins. Interestingly, the amino acid residue Arg415, which is altered in our patient, resides in the ETS DNA-binding domain. The proximity of the Arg415 residue to the DNA in our molecular modeling suggests that the mutation may interfere with the DNA binding of *ETV4* (Figure 2a). In addition, it has been previously shown that the charged residue Arg409 of *ETV1*, the equivalent of *ETV4* Arg415, could be involved in DNA binding through a salt bridge [25].

Thus, we investigated the effect of the Arg415His *ETV4* variant on DNA binding by electrophoretic mobility shift assay (EMSA) using a DNA probe containing a consensus ETS binding site. A shift in mobility of the labeled DNA probe was observed with 0.1nM of the wild-type *ETV4* ($K_d = 0.35 \pm 0.04$ nM), whereas no shift was detected after the addition of up to 12nM of the Arg415His *ETV4* mutant, suggesting that the p.Arg415His alteration fails to bind to its DNA sequence (Figure 2b).

To further test the DNA binding properties of the *ETV4* mutant, we performed a dual-luciferase reporter

assay in HEK293T cells. As shown in Figure 2c, the induced transcriptional activation of the Arg415His *ETV4* mutation was strongly reduced when compared to the wild-type *ETV4* ($P < 0.0001$), and did not differ significantly to that of the mock plasmid ($P = 0.8527$). The results therefore demonstrate an impairment of the Arg415His *ETV4* mutant in activating the transcription of a reporter gene. This most likely results from the loss of the DNA-binding activity and supports a loss-of-function hypothesis for the mutant *ETV4* (Figure 2b).

3.3. Wild-Type *ETV4* but not Arg415His Mutant Rescues Migration Defects in *ETV4* Knock-Down Cells

ETV4 has previously been linked to a wide variety of functions including the regulation of cell proliferation, cell differentiation, and cell migration in various tissues [15, 24]. In the developing kidney, *ETV4* is known as a downstream target of Ret and is required for normal development of the ureteric bud and the nephric duct [14, 17, 26]. Recent studies more specifically imply a role of *ETV4* in ureteric bud cell movement, and promotion of ureteric bud growth and branching

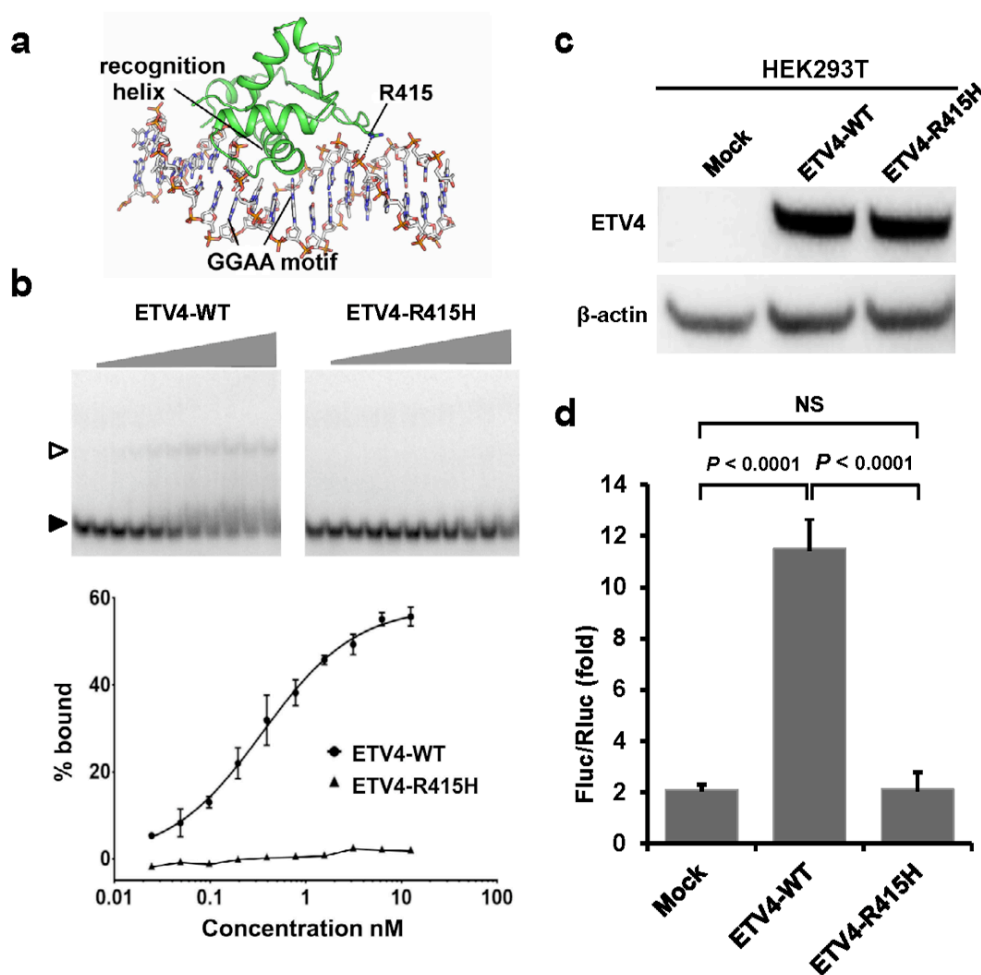


Figure 2: EMSA and dual-luciferase reporter assay demonstrate loss of DNA binding for *ETV4* variant p.Arg415His. (a) Molecular model of *ETV4* in complex with 18 bp duplex DNA suggests Arg415 forms a salt bridge (dotted black line) with the phosphate moiety 3 base pairs upstream of the GGAA recognition motif. The model was created by extending the *ETV4* 10bp DNA complex (PDBid 4UUV (15)) with canonical B-form DNA. (b) EMSA of the ETS domains for wild-type and Arg415His *ETV4*. Radio-labelled EBS DNA probe was incubated with the increasing concentrations of purified wild type of Arg415His mutant *ETV4* ETS domain (residues 338-435). The upper panel shows representative gels with open and closed triangles indicating the positions of the protein-bound and unbound probes, respectively. The lower panel shows quantification with data plotted as mean \pm SEM. (c and d) Results of *ETV4* luciferase assays and corresponding immunoblots. HEK293T cells were co-transfected with pGL3-5x*ETV4*-Luc reporter construct, pCS2 Renilla luciferase, and pRK5-N-Myc expression vector (empty vector), *ETV4* wild-type or *ETV4* Arg415His mutant). The upper panel (c) shows the corresponding Western blot analysis of *ETV4* levels in HEK293T cells (β -actin as a loading control). The lower panel (d) shows deficient transcriptional activation of *ETV4* Arg415His mutant. Relative Firefly luciferase activity was obtained after normalizing to Renilla luciferase activity. Data are presented as the means and standard deviations from two independent experiments with triplicate measurements. Differences in luciferase activity were assessed by a two-tailed Student t test. NS: not significant.

[14, 15, 24]. Deficiencies in either of these processes constitute known causes of CAKUT.

We therefore performed migration assays to assess a possible impact of the Arg415His *ETV4* variant on cell migration. Human PC3 and U-2 OS cells were chosen here, because cell lines generated from the human embryonic urinary system (e.g., HEK293T) were not considered suitable given the experimental setup, whereas these two cell lines have successfully been shown to exhibit *ETV4* dependent cell migration rates in the literature and were suitable for the scratch-wound migration assay [26].

The envisaged experimental setup of initial knock-down and subsequent visualization of a rescue vs. non-rescue effect *via* transfection of the wild type vs. mutant *ETV4* construct, respectively, made a stable *ETV4* knock-down cell-line preferable. Stable knock-down cells appeared to tolerate the following transfection of constructs better, with less impact on cell viability, and therefore had a more reliable and reproducible performance in the migration assay. However, this setup made the use of primary cell lines (e.g., ureteric bud cells) less feasible.

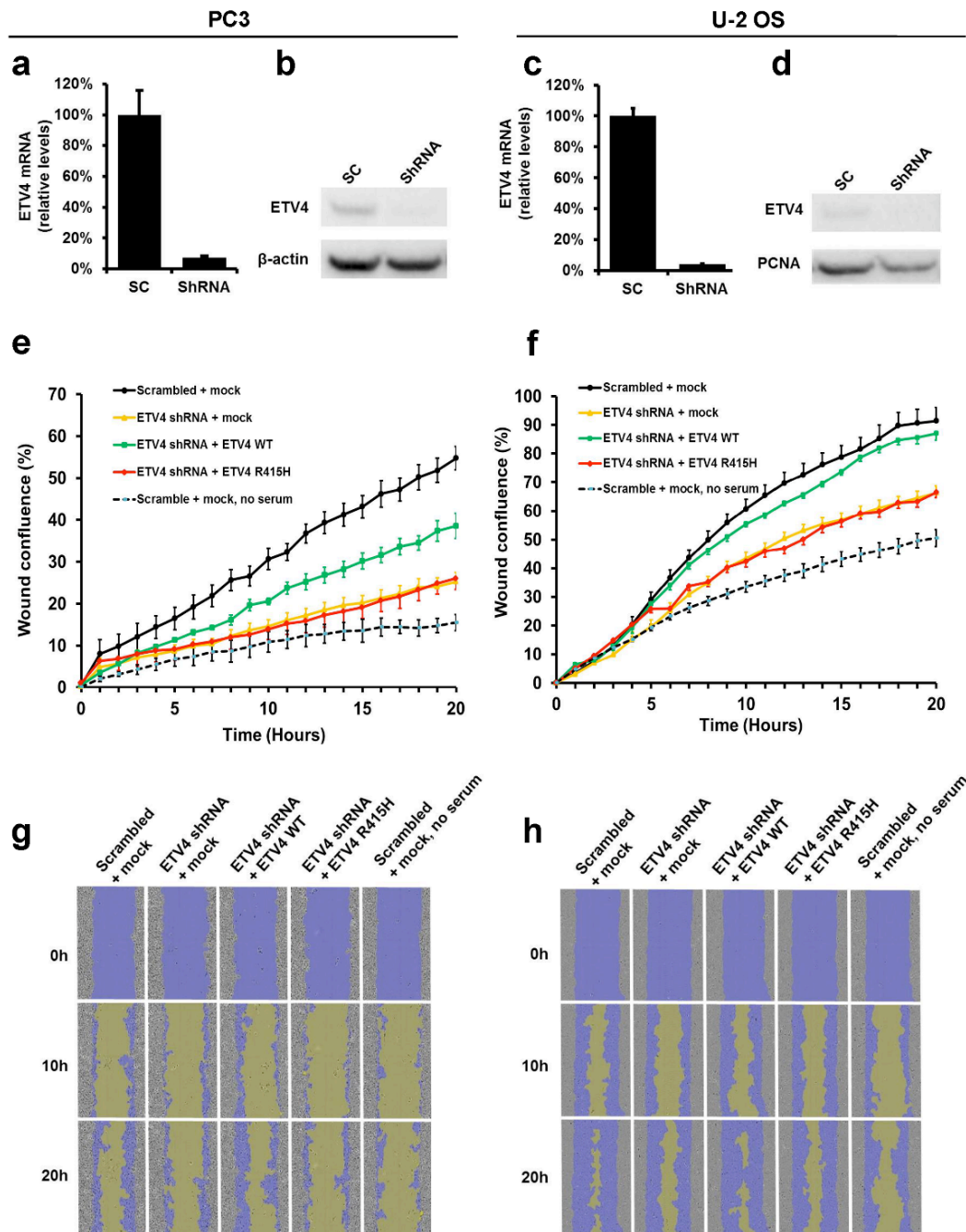


Figure 3: *ETV4* mutant p.Arg415His fails to rescue cell migration rate reduced by *ETV4* knock-down. All experiments were performed in the Incucyte system in two different cell lines, PC3 cells (up lay, **a, b, e, g**) and U-2 OS cells (down lay, **c, d, f, h**). (**a-d**) Efficient knock down of *ETV4* mRNA level, (**a, c**) and protein level, (**b, d**) in PC3 (**a, b**) and U-2 OS (**c, d**) cell lines, respectively. Cells were stably transduced with retroviral shRNA expression vectors encoding either a non-target control (scrambled) or *ETV4* shRNA. *ETV4* mRNA level (normalized to housekeeping gene *GAPDH*) was tested by quantitative real-time (qRT)-PCR. *ETV4*, β -actin, and PCNA protein levels were analyzed by Western blot. (**e** and **f**) Confluent monolayers were wounded using a semi-manual wound maker tool. Migration of cells was quantified based on images that were taken every hour for up to 20 hours. In PC3 (**e**) and U-2 OS (**f**) cells, knockdown of *ETV4* by using *ETV4* shRNA reduces cell migration (yellow versus black). Base line migration rate (dashed lines) is strongly increased upon addition of serum (solid black lines). The decrease in cell migration is partially rescued by transfection with full-length human *ETV4* cDNA (green lines), but not rescued by transfection with *ETV4* Arg415His mutant vector (red lines) or mock transfection (yellow lines). (**g** and **h**) Representative images are shown in PC3 cells (**g**) and U-2 OS cells (**h**).

An efficient knock-down of *ETV4* on both the mRNA and protein level was obtained *via* retroviral infection of

the target cell lines with an shRNA expression construct (Figure 3a-d). Human PC3 and U-2 OS cells

with stable depletion of endogenous human *ETV4* demonstrated a slower migration rate in comparison to non-target control cells (Figure 3e-h). This effect was rescued by a transfection with human N-myc *ETV4*-WT. However, stable *ETV4* knockdown cells transfected with cDNA construct N-myc-*ETV4*-Arg415His, that was present homozygously in patient B24-21 with CAKUT, remained to exhibit migratory deficiencies (Figure 3e-h).

This loss-of-function effect in the migration assay together with the insights gained from the EMSA and the luciferase assay give reason to speculate that the *ETV4* Arg415His mutation eliminates the expression of effector genes that participate in cell movement. Candidate genes include the chemokine receptor *Cxcr4* and the matrix metalloproteinase *Mmp14* [14]. This hypothesis however, would have to be further investigated with future projects.

4. DISCUSSION

In this study, we identified a homozygous missense mutation in *ETV4* in a consanguineous individual with isolated CAKUT. The discovered variant causes an amino acid substitution in the highly conserved Ets DNA-binding domain and has never been reported homozygously in population databases. At the biochemical level we demonstrate that the *ETV4* mutant lost its DNA binding property. It furthermore exhibits a loss-of-function effect in rescuing migration defects in two *ETV4* knock-down cell lines. Hence, we hypothesize that the detected homozygous missense variant in the *ETV4* gene causes the CAKUT phenotype in the patient of the present study.

The phenotype of the patient with the recessive *ETV4* missense mutation resembles the murine CAKUT phenotype, although much milder when compared to the severe renal phenotypes seen in a proportion of *ETV4* null mice, and most *ETV4*; *ETV5* compound mutant mice [14]. Furthermore, no extra-renal phenotypes, such as nervous system or limb malformations were seen, which have been described in *ETV4* [27] or *ETV4* [28]; *ETV5* compound knock-out mice, respectively. This discrepancy may be explained by a redundancy of *ETV4* with *ETV5* or other ETS proteins and/or alternative mechanisms of *ETV4* that work independently of the DNA-binding property [26, 29].

However, in view of the convincing *in vivo* data in the literature and the functional data presented here we hypothesize that the recessive mutation identified in *ETV4* causes the CAKUT phenotype seen in our patient, the most likely mechanism here by being an impairment of the GDNF/RET/*ETV4* signaling pathway.

DISCLOSURE

All the authors declare no competing interests.

ACKNOWLEDGEMENTS

We are grateful for the family who contributed to this study. We thank Prof. Andrew Sharrocks and Karren Palmer for providing us with the pGL3-5x*ETV4* luciferase reporter plasmid. We thank Cristina Cebrian for helpful discussions.

FH is a Warren E. Grupe Professor of Pediatrics. This work was supported by grants from the National Institutes of Health [DK088767 to FH; DK075578 to FC U54HG006504 to RPL and DK096238 to RSL]. OG and JAN are funded by the SGC, a registered charity [number 1097737] that receives funds from AbbVie, Bayer Pharma AG, Boehringer Ingelheim, the Canada Foundation for Innovation, Genome Canada, GlaxoSmithKline, Janssen, Lilly Canada, Merck and Co., the Novartis Research Foundation, the Ontario Ministry of Economic Development and Innovation, Pfizer, São Paulo Research Foundation-FAPESP, Takeda, and the Wellcome Trust [092809/Z/10/Z]. AvdV is supported by a Postdoctoral Research Fellowship of the German Research Foundation [VE916/1-1]. AV is a recipient of the Fulbright postdoctoral scholar award for 2013 and is also supported by grants from the Manton Center Fellowship Program, Boston Children's Hospital, Boston, Massachusetts, USA, and the Mallinckrodt Research Fellowship Award. EW is supported by the Leopoldina Fellowship Program, German National Academy of Sciences Leopoldina [LPDS 2015-07].

AUTHOR CONTRIBUTION

#These authors contributed equally to this work.

REFERENCES

- [1] Ichikawa I, Kuwayama F, Pope Jc, Stephens FD and Miyazaki Y. Paradigm shift from classic anatomic theories to contemporary cell biological views of CAKUT. *Kidney International* 2002; 61(3): 889-98. <https://doi.org/10.1046/j.1523-1755.2002.00188.x>

- [2] Pohl M, Bhatnagar V, Mendoza SA and Nigam SK. Toward an etiological classification of developmental disorders of the kidney and upper urinary tract. *Kidney International* 2002; 61(1): 10-9. <https://doi.org/10.1046/j.1523-1755.2002.00086.x>
- [3] Smith JM, Stablein DM, Munoz R, Hebert D and McDonald RA. Contributions of the Transplant Registry: The 2006 Annual Report of the North American Pediatric Renal Trials and Collaborative Studies (NAPRTCS). *Pediatric transplantation* 2007; 11(4): 366-73. <https://doi.org/10.1111/j.1399-3046.2007.00704.x>
- [4] Ingelfinger JR, Kalantar-Zadeh K and Schaefer F. World Kidney Day Steering C. *World Kidney Day* 2016: Averting the legacy of kidney disease-focus on childhood. *Pediatric nephrology* 2016; 31(3): 343-8. <https://doi.org/10.1007/s00467-015-3255-7>
- [5] Vivante A, Kohl S, Hwang DY, Dworschak GC and Hildebrandt F. Single-gene causes of congenital anomalies of the kidney and urinary tract (CAKUT) in humans. *Pediatric nephrology* 2014; 29(4): 695-704. <https://doi.org/10.1007/s00467-013-2684-4>
- [6] Vivante A and Hildebrandt F. Exploring the genetic basis of early-onset chronic kidney disease. *Nature reviews Nephrology* 2016; 12(3): 133-46. <https://doi.org/10.1038/nrneph.2015.205>
- [7] Humbert C, Silbermann F, Morar B, Parisot M, Zarhrate M, Masson C, et al. Integrin alpha 8 recessive mutations are responsible for bilateral renal agenesis in humans. *American journal of human genetics* 2014; 94(2): 288-94. <https://doi.org/10.1016/j.ajhg.2013.12.017>
- [8] Barak H, Huh SH, Chen S, Jeanpierre C, Martinovic J, Parisot M, et al. FGF9 and FGF20 maintain the stemness of nephron progenitors in mice and man. *Developmental cell* 2012; 22(6): 1191-207. <https://doi.org/10.1016/j.devcel.2012.04.018>
- [9] Vivante A, Kleppa MJ, Schulz J, Kohl S, Sharma A, Chen J, et al. Mutations in TBX18 Cause Dominant Urinary Tract Malformations via Transcriptional Dysregulation of Ureter Development. *American journal of human genetics* 2015; 97(2): 291-301. <https://doi.org/10.1016/j.ajhg.2015.07.001>
- [10] Hwang DY, Kohl S, Fan X, Vivante A, Chan S, Dworschak GC, et al. Mutations of the SLIT2-ROBO2 pathway genes SLIT2 and SRGAP1 confer risk for congenital anomalies of the kidney and urinary tract. *Human genetics* 2015; 134(8): 905-16. <https://doi.org/10.1007/s00439-015-1570-5>
- [11] Kohl S, Hwang DY, Dworschak GC, Hilger AC, Saisawat P, Vivante A, et al. Mild recessive mutations in six Fraser syndrome-related genes cause isolated congenital anomalies of the kidney and urinary tract. *Journal of the American Society of Nephrology: JASN* 2014; 25(9): 1917-22. <https://doi.org/10.1681/ASN.2013101103>
- [12] Saisawat P, Kohl S, Hilger AC, Hwang DY, Yung Gee H, Dworschak GC, et al. Whole-exome resequencing reveals recessive mutations in TRAP1 in individuals with CAKUT and VACTERL association. *Kidney international* 2014; 85(6): 1310-7. <https://doi.org/10.1038/ki.2013.417>
- [13] Cooper CD, Newman JA and Gileadi O. Recent advances in the structural molecular biology of Ets transcription factors: interactions, interfaces and inhibition. *Biochemical Society transactions* 2014; 42(1): 130-8. <https://doi.org/10.1042/BST20130227>
- [14] Lu BC, Cebrian C, Chi X, Kuure S, Kuo R, Bates CM, et al. ETV4 and ETV5 are required downstream of GDNF and Ret for kidney branching morphogenesis. *Nature genetics* 2009; 41(12): 1295-302. <https://doi.org/10.1038/ng.476>
- [15] Riccio P, Cebrian C, Zong H, Hippenmeyer S and Costantini F. Ret and ETV4 Promote Directed Movements of Progenitor Cells during Renal Branching Morphogenesis. *PLoS biology* 2016; 14(2): e1002382. <https://doi.org/10.1371/journal.pbio.1002382>
- [16] Marra AN and Wingert RA. Epithelial cell fate in the nephron tubule is mediated by the ETS transcription factors *etv5a* and *ETV4* during zebrafish kidney development. *Developmental biology* 2016; 411(2): 231-45. <https://doi.org/10.1016/j.ydbio.2016.01.035>
- [17] Braun DA, Sadowski CE, Kohl S, Lovric S, Astrinidis SA, Pabst WL, et al. Mutations in nuclear pore genes NUP93, NUP205 and XPO5 cause steroid-resistant nephrotic syndrome. *Nature genetics* 2016; 48(4): 457-65. <https://doi.org/10.1038/ng.3512>
- [18] Seelow D, Schuelke M, Hildebrandt F and Nurnberg P. HomozygosityMapper--an interactive approach to homozygosity mapping. *Nucleic acids research* 2009; 37(Web Server issue): W593-9.
- [19] Upadhyay S, Liu C, Chatterjee A, Hoque MO, Kim MS, Engles J, et al. LKB1/STK11 suppresses cyclooxygenase-2 induction and cellular invasion through PEA3 in lung cancer. *Cancer research* 2006; 66(16): 7870-9. <https://doi.org/10.1158/0008-5472.CAN-05-2902>
- [20] Huang WY, Xie W, Guo X, Li F, Jose PA and Chen SY. Smad2 and PEA3 cooperatively regulate transcription of response gene to complement 32 in TGF-beta-induced smooth muscle cell differentiation of neural crest cells. *American journal of physiology Cell physiology* 2011; 301(2): C499-506. <https://doi.org/10.1152/ajpcell.00480.2010>
- [21] Hwang DY, Dworschak GC, Kohl S, Saisawat P, Vivante A, Hilger AC, et al. Mutations in 12 known dominant disease-causing genes clarify many congenital anomalies of the kidney and urinary tract. *Kidney international* 2014; 85(6): 1429-33. <https://doi.org/10.1038/ki.2013.508>
- [22] Guo B, Panagiotaki N, Warwood S and Sharrocks AD. Dynamic modification of the ETS transcription factor PEA3 by sumoylation and p300-mediated acetylation. *Nucleic acids research* 2011; 39(15): 6403-13. <https://doi.org/10.1093/nar/gkr267>
- [23] Bojovic BB and Hassell JA. The PEA3 Ets transcription factor comprises multiple domains that regulate transactivation and DNA binding. *The Journal of biological chemistry* 2001; 276(6): 4509-21. <https://doi.org/10.1074/jbc.M005509200>
- [24] Kuure S, Chi X, Lu B and Costantini F. The transcription factors ETV4 and ETV5 mediate formation of the ureteric bud tip domain during kidney development. *Development* 2010; 137(12): 1975-9. <https://doi.org/10.1242/dev.051656>
- [25] Cooper CD, Newman JA, Aitkenhead H, Allerston CK and Gileadi O. Structures of the Ets Protein DNA-binding Domains of Transcription Factors ETV1, ETV4, ETV5, and Fev: Determinants of Dna Binding and Redox Regulation by Disulfide Bond Formation. *The Journal of biological chemistry* 2015; 290(22): 13692-709. <https://doi.org/10.1074/jbc.M115.646737>
- [26] Wollenick K, Hu J, Kristiansen G, Schraml P, Rehauer H, Berchner-Pfannschmidt U, et al. Synthetic transactivation screening reveals ETV4 as broad coactivator of hypoxia-inducible factor signaling. *Nucleic acids research* 2012; 40(5): 1928-43. <https://doi.org/10.1093/nar/gkr978>
- [27] Livet J, Sigrist M, Stroebel S, De Paola V, Price SR, Henderson CE, et al. ETS gene *Pea3* controls the central position and terminal arborization of specific motor neuron pools. *Neuron* 2002; 35(5): 877-92. [https://doi.org/10.1016/S0896-6273\(02\)00863-2](https://doi.org/10.1016/S0896-6273(02)00863-2)
- [28] Zhang Z, Verheyden JM, Hassell JA and Sun X. FGF-regulated ETV genes are essential for repressing Shh

expression in mouse limb buds. *Developmental cell* 2009; 16(4): 607-13.
<https://doi.org/10.1016/j.devcel.2009.02.008>

[29] Hollenhorst PC, McIntosh LP and Graves BJ. Genomic and biochemical insights into the specificity of ETS transcription factors. *Annual review of biochemistry* 2011; 80: 437-71.
<https://doi.org/10.1146/annurev.biochem.79.081507.103945>

Received on 08-12-2016

Accepted on 19-12-2016

Published on 31-12-2016

DOI: <http://dx.doi.org/10.12974/2311-8687.2016.04.02.1>

© 2016 Jing *et al.*; Licensee Savvy Science Publisher.

This is an open access article licensed under the terms of the Creative Commons Attribution Non-Commercial License (<http://creativecommons.org/licenses/by-nc/3.0/>) which permits unrestricted, non-commercial use, distribution and reproduction in any medium, provided the work is properly cited.